

## The Role of Mediobasal Hypothalamic PACAP in the Control of Body Weight and Metabolism

Nadejda Bozadjieva-Kramer<sup>1\*</sup>, Rachel A. Ross<sup>2,3,4\*</sup>, David Q. Johnson<sup>5</sup>, Henning Fenselau<sup>3,6,7,8</sup>, David L. Haggerty<sup>9</sup>, Brady Atwood<sup>9</sup>, Bradford Lowell<sup>3,4</sup>, Jonathan N. Flak<sup>5,9,10</sup>

\*These authors contributed equally

<sup>1</sup>Department of Surgery, University of Michigan, Ann Arbor, MI, USA

<sup>2</sup>Albert Einstein College of Medicine, Bronx, NY, USA

<sup>3</sup>Beth Israel Deaconess Medical Center, Boston, MA, USA,

<sup>4</sup>Harvard Medical School, Boston, MA, USA,

<sup>5</sup>Indiana Biosciences Research Institute, Diabetes Research Center, Indianapolis, IN, USA

<sup>6</sup>Synaptic Transmission in Energy Homeostasis Group, Max Planck Institute for Metabolism Research, Gleueler Strasse 50, 50931 Cologne, Germany

<sup>7</sup>Center for Endocrinology, Diabetes and Preventive Medicine (CEDP), University Hospital Cologne, Kerpener Strasse 26, 50924 Cologne, Germany

<sup>8</sup>Excellence Cluster on Cellular Stress Responses in Aging Associated Diseases (CECAD) and Center of Molecular Medicine Cologne (CMMC), University of Cologne, Cologne, Germany.

<sup>9</sup>Indiana University School of Medicine, Pharmacology and Toxicology, Indianapolis, IN, USA

<sup>10</sup>Department of Internal Medicine, Division of Metabolism, Endocrinology, and Diabetes, University of Michigan, Ann Arbor, MI, USA

Correspondence:

Jonathan N. Flak, PhD

Indiana Biosciences Research Institute

1345 W. 16<sup>th</sup> Street

Indianapolis, IN 46022

Phone: 317-983-3315

Fax: 317-983-3350

Email: [jflak@indianabiosciences.org](mailto:jflak@indianabiosciences.org)

Reprint requests should be addressed to Jonathan N. Flak, PhD

Support:

NIH (P30 DK046200, P30 DK057521, R01 DK075632, R01 DK089044, R01 DK096010, R01 DK111401 to BL, 5T32DK108740 and UL1TR002240 to NBK, K08 DK118201 and T32 HL007374 to RR, and 5T32AA007462 to DLH)

The American Diabetes Association (17-INI-15 to JNF)

Accepted Manuscript

## Abstract

Body energy homeostasis results from balancing energy intake and energy expenditure. Central nervous system administration of pituitary adenylate cyclase activating polypeptide (PACAP) dramatically alters metabolic function, but the physiologic mechanism of this neuropeptide remains poorly defined. PACAP is expressed in the mediobasal hypothalamus (MBH), a brain area essential for energy balance. Ventromedial hypothalamic nucleus (VMN) neurons contain, by far, the largest and most dense population of PACAP in the medial hypothalamus. This region is involved in coordinating the sympathetic nervous system in response to metabolic cues in order to re-establish energy homeostasis. Additionally, the metabolic cue of leptin signaling in the VMN regulates PACAP expression. We hypothesized that PACAP may play a role in the various effector systems of energy homeostasis, and tested its role by using VMN-directed, but MBH encompassing, AAV<sup>Cre</sup> injections to ablate *Adcyap1* (gene coding for PACAP) in mice (*Adcyap1*<sup>MBH</sup> KO mice). *Adcyap1*<sup>MBH</sup> KO mice rapidly gained body weight and adiposity, becoming hyperinsulinemic and hyperglycemic. *Adcyap1*<sup>MBH</sup> KO mice exhibited decreased oxygen consumption (VO<sub>2</sub>), without changes in activity. These effects appear to be due at least in part to BAT dysfunction, and we show that PACAP-expressing cells in the MBH can stimulate BAT thermogenesis. While we observed disruption of glucose clearance during hyperinsulinemic/euglycemic clamp studies in obese *Adcyap1*<sup>MBH</sup> KO mice, these parameters were normal prior to the onset of obesity. Thus, MBH PACAP plays important roles in the regulation of metabolic rate and energy balance through multiple effector systems on multiple time scales, which highlight the diverse set of functions for PACAP in overall energy homeostasis.

### Keywords:

Energy expenditure, Energy balance, ventromedial hypothalamus, thermogenesis, glucose homeostasis, obesity

## Introduction

The health morbidities due to obesity cost approximately \$150 billion annually in the United States underscoring the need to alleviate this burden (1,2). Treatments that globally activate the sympathetic nervous system (SNS) increase metabolic rate and promote weight loss, but also cause dangerous cardiovascular and psychiatric side effects (3-5). Therefore, a better understanding of the specific mechanisms that govern energy balance will lead to safer and more effective weight loss interventions.

The central nervous system (CNS) is uniquely positioned to promote energy balance in the context of a range of experiential and environmental signals sensed by the brain (e.g. famine, illness, injury) (6,7). The brain uses a collection of neurotransmitters, many of them in the form of neuropeptides, that provide important roles in sustaining lasting effects on synaptic function. One such neuropeptide is pituitary adenylate cyclase activating polypeptide (PACAP) (8). PACAP (encoded by gene *Adcyap1*) through direct action on its receptor, PACAP Receptor 1 (PAC1R) (9), increases sympathetic activity at peripheral targets (9-11), stimulating glucose production (12) and energy expenditure in mice (8,13,14). While pharmacological administration of PACAP provides these positive metabolic responses that would predict an important role in improved energy balance, knockouts of either PACAP or PAC1R are not obese, but have significant issues in surviving post-natal weaning (15,16). These reports have suggested a multifaceted role for PACAP across development.

PACAP is expressed in the periphery and CNS, but the distinct role of tissue-specific PACAP remains undefined. The mediobasal hypothalamus (MBH) contains a pronounced collection of PACAP-containing cells in the ventromedial hypothalamic nucleus (VMN), a nucleus that plays crucial roles in modulating SNS activation to regulate blood glucose, thermogenesis, energy expenditure, and food intake. VMN neurons stimulate these responses through the release of neurotransmitters

at a downstream neural site (17,18). Introducing light chain tetanus toxin, in order to prevent vesicular communication, into VMN steroidogenic factor 1 (SF1) cells, but not Cholecystokinin Receptor B (CCKBR)-containing cells, results in obesity and reduced oxygen consumption (19). This indicates that communication by specific VMN cells that do not contain CCKBR is necessary for energy balance (19). Leptin and fasting both modulate *Adcyap1* expression in the VMN, but not elsewhere in the CNS (8). Furthermore, leptin action in VMN cells is essential for energy balance via the facilitation of energy expenditure (20). Taken together, these data implicate that both the VMN and the neuropeptide PACAP are important in the regulation of energy balance. However, the specific functions for PACAP within the VMN in the regulation of metabolic parameters remain unclear.

In these studies, we tested the necessity for mediobasal hypothalamic (MBH) PACAP in normal energy balance and glycemic control, the two main functions by which PACAP is proposed to influence metabolism in this region. We used VMN-directed, but MBH encompassing, AAV<sup>Cre</sup> injections to ablate *Adcyap1* (gene coding for PACAP) in *Adcyap1<sup>flox</sup>* mice (*Adcyap1<sup>MBH</sup>KO* mice). *Adcyap1<sup>MBH</sup>KO* mice rapidly gained body weight and adiposity on a standard chow, and became hyperinsulinemic and hyperglycemic. *Adcyap1<sup>MBH</sup>KO* mice exhibited decreased oxygen consumption (VO<sub>2</sub>), carbon dioxide production (VCO<sub>2</sub>), and respiratory exchange ratio (RER), without changes in activity, resulting in severe obesity. Unexpectedly, these mice also showed increased brown adipose tissue weight and upregulated markers of fat oxidation. While we observed slightly increased feeding and disruption of glucose clearance during hyperinsulinemic/euglycemic clamp studies in obese *Adcyap1<sup>MBH</sup>KO* mice, these parameters were normal prior to the onset of obesity. Thus, feeding only played a modest role in sustaining obesity. Our studies showed that MBH PACAP plays important roles in the regulation of metabolic rate and energy balance through multiple effector pathways on multiple time scales, but is not required for direct modulation of food intake or glucose homeostasis.

## Materials and Methods

**Animals.** The procedures included in this manuscript were approved by the Committee on the Use and Care of Animals at the University of Michigan (Ann Arbor, MI), Beth Israel Deaconess Medical Center (Boston, MA), and Indiana University (Indianapolis, IN). All mice were provided with standard chow and water *ad libitum*, unless noted otherwise, and kept in a temperature-controlled (22°C) room on a 12-hour light-dark cycle. *Adcyap1<sup>fllox</sup>* mice were generated by R.A.R. and B.B. (21). The two loxp sites flank the second exon of the *Adcyap* gene. When recombined, this creates a frameshift mutation and results in a truncated, nonfunctional PACAP protein (21). All experiments were carried out using approximately equal numbers of male and female mice. Experimental design and animals used are outlined in Supplemental Figure 1 (22). Mice were single-housed for BAT temperature recording. Mice were group-housed prior to stereotaxic surgery in all cohorts, but single-housed post-operatively in cohorts 1 and 2 for food intake studies. Exactly 8 GFP and 11 Cre were used in cohorts 1 (male) and 2 (female). In cohort 3, 5 GFP and 7 Cre male mice were used. In cohort 4, 5 GFP (3 Male, 2 Female) and 7 Cre (4 Male, 3 Female) were used. Unless stated, male and female mice were included for the analysis. Investigators were blinded to the treatment for all studies. All mice were genotyped via polymerase chain reaction (PCR) across the genomic region of interest prior to study (21) and only mice homozygote for *Adcyap1<sup>fllox</sup>* or *Adcyap1<sup>cre</sup>* were included in the study. All mice were bred via in-house colonies.

**Phenotypic Studies.** Body weight and food intake were monitored weekly in all mice post-surgery. Body weight and food were weighed weekly on an Ohaus NV511 precision balance (Parsippany, NJ). Mice were single housed after surgery for food intake measurement, but mice were group housed for studies that only included either glucose clamps or indirect calorimetry. Glycemic measures (including intraperitoneal (IP) glucose tolerance test (GTT; 2g/kg body weight, IP) and insulin tolerance test (ITT; 0.6 Unit/kg body weight, Humulin (Eli Lilly), IP) were performed in 12-18-week-

old animals. Blood glucose was measured with a One Touch Ultra 2 glucometer (Johnson and Johnson) by tail vein draw. For all glycemic measures, mice were fasted for 4-6 hours prior to testing. Body fat and lean mass were analyzed in a cohort of mice using Minispec LF9011 (Bruker Optics, Billerica, MA). Body composition data was collected with assistance from Indiana University School of Medicine Mouse Metabolic Phenotyping Center. TSE Phenomaster cages were used for indirect calorimetry measurement, with assistance from the Indiana University School of Medicine Mouse Metabolic Phenotyping Center. Indirect calorimetry data was used to calculate fat oxidation and glucose oxidation via the Weir equation (23). Data were analyzed by taking into account whole body mass and lean mass separately. Glucagon, insulin, and leptin were all assayed in plasma by commercial enzyme-linked immunosorbent assays (Glucagon: Mercodia, Uppsala, Sweden, RRID: AB\_2783839 (24); Leptin: Crystal Chem, Elk Grove, IL; RRID: AB\_2722664 (25); Insulin: Crystal Chem, Elk Grove, IL; RRID: AB\_2783626 (26)). Corticosterone was measured with radioimmunoassay (MP Biomedicals, Santa Ana, California, RRID: AB\_2801269 (27)) with assistance from the Chemistry Core supported by the Michigan Diabetes Research Center (University of Michigan).

**Reagents.** All AAVs used include titer from stock. AAV-Cre-GFP ( $1.1 \times 10^{13}$  GC/ml), from Addgene plasmid 68544, was generated in at the University of Michigan Viral Vector Core with the support of the Molecular Genetics Core of the Michigan Diabetes Research Center (University of Michigan, Ann Arbor, Michigan, USA) or directly acquired from Addgene ( $2.7 \times 10^{13}$  GC/ml) (105540). AAV-GFP ( $5.4 \times 10^{12}$  GC/ml) was acquired from the University of North Carolina Vector Core (6765) or Addgene ( $3.4 \times 10^{13}$  GC/ml) (105539). It is important to note that the two AAV-Cre used have different promoters. Addgene 68544 has a CMV, whereas 105540 has a hSyn promoter. All of these AAVs were serotype 9.

**Hyperinsulinemic-euglycemic clamp.** In both cohorts, only male mice were used for hyperinsulinemic-euglycemic clamps. In the first cohort, mice were catheterized (arterial and venous) at 11 weeks post-stereotaxic injection, while mice were catheterized 3 weeks post-injection in the second cohort. Mice were allowed to recover from surgery and only went through the clamping procedure if the animals had no sign of being sick or ill. After a 5-hour fast, conscious, unstressed, catheterized mice were infused with 10mU/kg/minute insulin, and glucose was clamped at ~150mg/dl for 120 minutes. After clamp, mice were administered (venous catheter) with [<sup>14</sup>C]-labeled 2 Deoxy-D-Glucose (2DG). Organs were collected for radioactivity measurements as a marker for glucose uptake, as previously described (28).

**Brown Adipose Tissue Temperature.** Temperature probes were surgically implanted directly above the interscapular brown adipose tissue (as previously described (29)) in PACAP-2a-cre mice (as previously described (30)) that received AAV-DIO-hM3dq into the VMN at the Beth Israel Deaconess Medical Center. Animals were allowed 1-week recovery and acclimation was performed with saline injection for 5 consecutive days. Data were collected using a handheld reader system (DAS-7006/7r; Bio Medic Data System) at the time points indicated.

**Stereotaxic Injections of Viral Constructs.** 8-14-week old animals were anesthetized with 1.5-2% isoflurane, in preparation for craniotomy. 15-18 week old mice were used in cohort 3 because it was a short term study compared to cohorts 1 and 2. After exposing the skull, bregma and lambda were leveled, a hole was drilled, and the contents of a pulled pipette at the coordinates of our target for ~25nl/min were released. For the VMN-directed injections, 100nl of virus was injected at anteroposterior (AP) -1.05 and -1.15, mediolateral (ML) +/- 0.3, dorsoventral (DV) -5.55. Four total injections (two on each side within the same drilled hole for a total of 200 nl per side) were

administered per animal, in order to spread the virus throughout the full extent of the VMN and get almost complete knockdown throughout the nucleus. We allowed at least 5 minutes for the virus to diffuse into the brain and the pipette was raised slowly out of the hole in the skull. The hole in the skull was filled with bone wax, and the skin was closed with surgical sutures (Henry Schein). Analgesics (Carprofen, 5mg/kg) were administered prophylactically to all mice to prevent post-surgical pain. The animals were allowed four weeks to recover from surgery before any experimental manipulation. For food intake studies, the animals were individually housed post-surgery in order to collect food intake data. Otherwise, animals continued to be housed with littermates. GFP fluorescent reporters in all studies were used to confirm proper targeting of the brain region. If bilateral fluorescence was not observed within the dmVMN, these cases were omitted from analyses.

**Perfusion and Immunohistochemistry.** Brains were collected and processed as previously described (31,32). Mice were anesthetized with isoflurane prior to transcardial perfusion with phosphate buffered saline (PBS) followed by 10% neutral buffered formalin (NBF) (Sigma Aldrich). Brains were removed and placed into 10% NBF overnight, followed by 30% sucrose for at least 36 hours. Brains were cut into 30  $\mu$ m sections on a freezing microtome in four series and stored in antifreeze solution (25% ethylene glycol, 25% glycerol). Sections were washed with PBS and then treated sequentially with 1% hydrogen peroxide/ 0.5% sodium hydroxide, 0.3% glycine, and 0.03% sodium dodecyl sulfate. Pretreatment was followed by an hour in blocking solution (PBS containing 0.1% triton, 3% Normal Donkey Serum), followed by overnight incubation in blocking solution containing either chicken anti-GFP (GFP-1020, RRID:AB\_1000240 (33), Aves, 1:1000), rabbit anti-NeuN (ABN78, RRID:AB\_10807945 (34), Millipore, 1:500), or rat anti-mCherry (Life Technologies M11217, RRID:AB\_2307319, 1:1,000 (35)). The next day, the sections were incubated with fluorescent

secondary antibodies (Molecular Probes, 1:200). The sections were mounted onto slides coverslipped with Fluoromount-G containing DAPI (Southern Biotech).

**In Situ Hybridization.** In situ hybridization for *Adcyap1* was performed in perfused brain tissue, using DEPC-treated PBS and 30% sucrose solution. Once the brains sunk in the 30% sucrose solution at 4°C, brains were sectioned on a freezing stage microtome at 30µm increments. Series of brain sections were mounted onto SuperFrost plus slides (Fisher Scientific) then stored in a slide box at -20 °C. Slides were fixed in 10% NBF (Sigma Aldrich) for 20 minutes and subsequently dehydrated in increasing concentrations of ethanol, cleared in xylenes, rehydrated in decreasing concentrations of ethanol, and finally placed in pre-warmed sodium citrate buffer (pH 6.0). The slides were then microwaved for 10 minutes followed by dehydration in increasing concentration of ethanol. The slides were allowed to air-dry for at least 1 hour. The *Adcyap1* cDNA (template) was produced from mouse hypothalamic RNA. The following primers were used to amplify a 509 base pair sequence in the encoding region of the *Adcyap1* gene with polymerase promoters: F (T3) 5'-(CAG AGA TGC AAT TAA CCC TCA CTA AAG GGA GA) ACC ATG TGT AGC GGA GCA AG-3'; R (T7) 5'-(CCA AGC CCT CTA ATA CGA CTC ACT ATA GGG AGA) CGG CGT CCT TTG TTT TTA ACC-3'. Primers were acquired from Integrated DNA Technologies (IDT; Iowa). The *Adcyap1* riboprobe was generated by *in vitro* transcription using 35S-UTP as the radioisotope. Labeled riboprobe was diluted in hybridization solution and brain sections were hybridized overnight at 58 °C. The following day, sections were incubated in 0.002% RNase A followed by stringency washes. Sections were dehydrated in increasing concentrations of ethanol, air-dried,

and placed in X-ray film cassettes with BMR-2 film (Kodak, Rochester, NY, USA) for two days.

**Quantitative Real-Time PCR.** RNA was extracted from brown adipose tissue using RNeasy Lipid Tissue Mini kit (Qiagen). cDNA was synthesized by reverse transcription from mRNA using the iScript cDNA Synthesis Kit (Bio-Rad). Gene expression was performed by quantitative real time RT-PCR using Taqman gene expression assays using StepOnePlus detection system (Applied Biosystems) with a standard protocol. Relative abundance for each transcript was calculated by a standard curve of cycle thresholds and normalized to RL32.

**Cell Counts.** Images from 30 $\mu$ m thick sections containing Cy3 tagged NeuN were collected in the mediobasal hypothalamus using a Keyence BZ-X810 microscope with a 20X objective. The ventromedial hypothalamus (VMN) was identified by overlaying the corresponding bregma level from an anatomical reference atlas (Allen Mouse Brain Atlas) on microscope images in ImageJ. Two regions of interest (ROI) encompassing the whole VMN were drawn bilaterally for each microscope image and the ROI areas (pixel/inch<sup>2</sup>) were measured. Image thresholding (Otsu Method) followed by watershed segmentation was performed to determine the number of NeuN positive cells within each ROI. Data were reported as NeuN positive cells by ROI area to correct for bregma level differences in ROI size. Both right and left sides of the VMN were averaged for a final value.

**Statistics.** Our sample sizes are similar to previously published studies using similar approaches (32,36-39). Time-course blood glucose, body weight, and food intake data were analyzed by two-way repeated measures ANOVA with Fisher's LSD post hoc test. Data in Figure 1, 2B,F, 3A-C, 4G-H, 5E-I, and 6A-C, H-L were analyzed by student's t-test. Data in Figure 2A, C-D, E, G-H, 3D-S, 4A-F, 5A-D, and 6D-G were analyzed by two-way ANOVA. No data were removed unless the injection missed

the VMN or the animal was sick or injured at the time of the experiment (loss of > 10% body weight). Significance was set at  $p \leq 0.05$ . All data were analyzed using Prism (GraphPad, La Jolla, California).

## Results

### **VMN *Adcyap1* cells can elevate brown adipose tissue temperature**

Previous studies have linked VMN PACAP neurons with circulating glucose and insulin regulation (40), but none have investigated a direct role of VMN PACAP neurons in the regulation of energy expenditure. Due to the wide amount of data available that link the VMN with BAT function (41-44), we investigated whether VMN *Adcyap1* cells contributed to this function. We administered AAV<sup>DIO-hM3dq</sup> into the VMN of *Adcyap1-cre* knockin mice and monitored brown fat temperature with probes implanted directly above the interscapular brown adipose tissue. After clozapine-n-oxide (CNO) administration, brown adipose tissue temperature rapidly increased 1-2 degrees Celsius throughout a 4-hour trial, which did not happen when mice were treated with saline ( $F(2,8)=8.818$ ,  $p=0.0015$ ) (Figure 1A-B). These data support the hypothesis that VMN PACAP cells can influence whole body energy expenditure through brown adipose tissue thermogenesis, and directed our investigation to further discern the role of PACAP in this region to influence various modalities of energy balance.

### **AAV<sup>Cre</sup> injection ablates VMN *Adcyap1* expression**

We tested the hypothesis that *Adcyap1* in the VMN directly regulates energy expenditure and glucose metabolism by ablating *Adcyap1* expression in the VMN. We conditionally ablated *Adcyap1* in the VMN via microinjection of AAV<sup>Cre</sup> into the VMN of 8-14 week old *Adcyap1<sup>fllox</sup>* mice (21). By using this approach, we avoided the drawback of potentially eliminating PACAP outside of the brain using transgenic Cre mouse models (such as SF1<sup>CRE</sup>) that also target cells in peripheral tissues. PACAP is a peptide expressed throughout the periphery and the SF1<sup>Cre</sup> mouse model would induce Cre activity within some peripheral tissues (45).

Indeed, *Adcyap1* mRNA was present within areas known to contain the neuropeptide (e.g. cortex, preoptic area (POA), medial amygdala (MeA), ventral premammillary nucleus (PMV)), but was almost completely ablated from the dmVMN of all AAV<sup>Cre</sup>-injected mice (Figure 2A-C). In support of this qualitative evidence, we also quantified expression level from the films to confirm reduction in *Adcyap1* in the VMN ( $t(36)=13.26$ ,  $p<0.0001$ ) following injection of AAV<sup>Cre</sup>, but not within nearby areas such as the MeA, PMV, and POA (Figure 2A-C). AAV<sup>Cre</sup> injection contained a GFP tag, in order to observe the spread of the virus. All included cases contained bilateral GFP expression throughout the VMN. Injection was not completely confined in the VMN and did spread to some degree into nearby areas in order to induce desired near complete ablation of *Adcyap1* mRNA in the VMN. Of note, GFP cells were observed in the posterior hypothalamus (PH), arcuate nucleus, anterior hypothalamus (AHA), suprachiasmatic nucleus (SCN), and dorsomedial hypothalamus (DMH), depending on the injection site (Supp Fig 1) (22). Importantly, we did not observe PACAP mRNA expression above background in any of these regions, though it is known that small populations of PACAP expressing cells are found in much of the hypothalamus across development (46,47). Furthermore, unlike our VMN directed ablations, none of the other regions had the same localization of viral spread, which we use as indirect readout of PACAP-ablation across multiple mice. Therefore, while PACAP may have been ablated from these nearby regions if expressed there, it is unlikely that the loss of function we see across our metabolic tests in adult mice can be attributed to these regions other than the VMN. While AAVs have been used for many years without cytotoxic consequences, we wanted to ensure that we did not lesion the hypothalamus with our injections. DAPI-labeled nuclei were observed in a similar distribution in all groups (data not shown). To quantify this expression, we used NeuN as a biomarker for neurons. In the VMN, there was no difference in the density of cells in the VMN (Figure 2D-F). Therefore, AAV<sup>Cre</sup> sufficiently ablated PACAP from the VMN without lesioning the nucleus.

### **Loss of *Adcyap1* in MBH induces obesity in both male and female mice**

Experiments were designed to assess the function for MBH PACAP in metabolic function (see experimental design in Supp Fig 1) (22). *Adcyap1*<sup>MBH</sup>*KO* mice were noticeably larger than littermate/cagemate controls beginning at 8 weeks post-injection. As such, body weight was closely monitored in these mice for the duration and in subsequent cohorts of mice. Body weight steadily increased to almost 40% more than control mice 8 weeks post-surgery. This increase in body weight was observed in both male and in female mice (Figure 3A, Supp Fig 3A) ( $F(2,17)=10.2$ ,  $p<0.0001$ ) ( $F(2,17)=14.59$ ,  $p<0.0001$ ) with only a delayed and modest increase in food intake (Figure 3B, Supp Fig 3B) ( $F(2,17)=0.5095$ ,  $p=.0367$ ) ( $F(2,17)=.3172$ ,  $p=.1513$ ) (22). Because there was a mild increase in food intake starting at week 7, we measured the food intake in mice following a 24-hour fast at 10 weeks post-injection. However, fasting/re-feeding food intake responses were normal in these mice, indicating that feeding responses were only modestly affected after the onset of obesity (Figure 3C, Supp Fig 3C) (22). Since effects were similar across sexes, data was combined for subsequent analyses of indirect calorimetry and glycemic regulation.

### ***Adcyap1*<sup>MBH</sup>*KO* mice display dysfunctions in energy expenditure**

In order to perform indirect calorimetry measurements, we included a separate cohort of mice that were exposed to the metabolic chambers early into the process of the mice becoming obese (4 weeks post-injection). These mice did exhibit increased fat mass ( $t(11)=4.474$ ,  $p=0.0008$ ), but lean mass was not different compared to controls. (Figure 4A-B). Oxygen consumption,  $VO_2$  ( $F(2,10)=25.94$ ,  $p=0.0301$ ) and carbon dioxide production,  $VCO_2$  ( $F(2,10)=27.07$ ,  $p=0.0185$ ) were both reduced when normalized with lean mass, ((Figure 4E-F, G-H). Respiratory exchange ratio (RER) was also reduced ( $F(2,10)=26.99$ ,  $p=0.0076$ ) during the dark cycle (Figure 4M-N) *Adcyap1*<sup>MBH</sup>*KO* mice. Finally, fat oxidation was elevated ( $F(2,10)=4.979$ ,  $p=0.0051$ ) and glucose oxidation reduced (( $F(2,10)=5.06$ ,  $p=0.0029$ ) during the dark cycle (Figure 3P-S) in *Adcyap1*<sup>MBH</sup>*KO* mice. Certainly,

*Adcyap1*<sup>MBH</sup> KO mice exhibit dysfunctions in underlying metabolic activity, consistent with reduced energy expenditure. Therefore, the marked increase in body weight in the *Adcyap1*<sup>MBH</sup> KO mice were due to the metabolic dysfunctions in energy expenditure, and the delayed increase in food intake is likely secondary to changes in energy utilization.

**Obese *Adcyap1*<sup>MBH</sup> KO mice have increased iBAT weight and markers for lipid oxidation.**

Upon sacrificing the mice after indirect calorimetry experiments (5 weeks post-injection), we noticed that the *Adcyap1*<sup>MBH</sup> KO mice had considerably more interscapular brown adipose tissue (iBAT) than the controls (Figure 4C). Indeed, iBAT weights were over four times larger than controls. We next measured expression of targets in BAT tissue associated with thermogenesis and lipid oxidation (Supp Fig 4A-E) (22). Indeed, mitochondrial uncoupling protein 2 (*UCP2*) (t(12)=2.319, p=0.0267), Iodothyronine Deiodinase 2 (*DIO2*) (t(12)=2.157, p=0.0315), and Peroxisome proliferator-activated receptor gamma coactivator 1-alpha (*PGC1 $\alpha$* ) (t(12)=2.832, p=0.011) were all increased in the knockouts compared to the controls. However, we did not observe any differences in mitochondrial uncoupling protein 1 (*UCP1*) and PR domain containing 16 (*PRDM16*). These data, taken together with the indirect calorimetry, indicate that these obese mice are metabolically inflexible and utilize lipids rather than carbohydrates for energy, which may further contribute to their obese phenotype.

**Obese *Adcyap1*<sup>MBH</sup> KO mice are hyperglycemic and hyperinsulinemic, yet remain insulin tolerant**

In addition to influencing energy expenditure, PACAP plays a critical role in energy mobilization and glucose clearance into peripheral tissues. Thus, we tested whether loss of PACAP in the MBH leads to hyperglycemia and decreased glucose tolerance. In support of this hypothesis, we observed that *Adcyap1*<sup>MBH</sup> KO mice had higher fed and fasted (24 hours) blood glucose levels compared to the controls (F(1,38)=20.16, p<0.0001) (Figure 5A). In addition to hyperglycemia, *Adcyap1*<sup>MBH</sup> KO mice were hyperinsulinemic (F(1,75)=16.49, p=0.0001), but neither hyperglucagonemic nor

hypercortisolemic at either fasting or fed states (Figure 5B-D). The *Adcyap1*<sup>MBH</sup>*KO* mice also had impaired glucose tolerance ( $F(1,39)=6.504$ ,  $p=0.0148$ ) (Figure 5E). Despite of increased body weight and adiposity in addition to impaired glucose tolerance, *Adcyap1*<sup>MBH</sup>*KO* mice were not insulin resistant (Figure 5F). *Adcyap1*<sup>MBH</sup>*KO* mice had a comparable decrease in blood glucose levels as controls in response to exogenous insulin administration (0.6 Units/kg; Figure 5F). Glucagon and corticosterone levels 30 minutes post-insulin injection were not different between the groups (Figure 5G,H). Therefore, loss of PACAP in the MBH resulted in glucose intolerance, despite having normal insulin tolerance and counterregulatory responses.

### **Obese *Adcyap1*<sup>MBH</sup>*KO* mice have impaired glucose clearance**

In order to evaluate glucose clearance independent from changes in circulating insulin and glucose, we evaluated glucoregulation in *Adcyap1*<sup>MBH</sup>*KO* in a hyperinsulinemic/euglycemic condition. Blood glucose (12 weeks post-injection) was clamped at 150 mg/dl (Figure 6A). Considerably less glucose was infused in order to sustain equivalent circulating glucose levels in *Adcyap1*<sup>MBH</sup>*KO* compared to control mice ( $F(1,16)=24.28$ ,  $p=0.0002$ ) (Figure 6B). Indeed, hepatic glucose production ( $F(1,32)=6.28$ ,  $p=0.0175$ ) and insulin clearance ( $t(16)=5.845$ ,  $p<0.0001$ ) were also lower following the clamp, potentially contributing to the hyperglycemia in *Adcyap1*<sup>MBH</sup>*KO* mice (Figure 6C-D). At the end of the clamp, [<sup>14</sup>C] 2DG was infused and organs collected. Measured radioactivity was lower in the gastrocnemius muscle ( $t(16)=2.722$ ,  $p=0.0075$ ), heart ( $t(16)=3.872$ ,  $p=0.0007$ ), brown adipose tissue ( $t(16)=6.182$ ,  $p<0.0001$ ), subcutaneous fat ( $t(15)=3.913$ ,  $p=0.0007$ ), but not visceral fat of *Adcyap1*<sup>MBH</sup>*KO* mice (Figure 6E-I). Overall, these data suggest that, in addition to the control of adiposity and energy expenditure, loss of MBH PACAP results in hyperglycemia and diminished glucose clearance consistent with aberrant glucose specific regulation in the obese state.

### ***Adcyap1*<sup>MBH</sup> KO mice do not have impaired glucose clearance 4 weeks post-injection**

At 12 weeks post-injection, *Adcyap1*<sup>MBH</sup> KO mice are obese and thereby difficult to distinguish between the direct function of MBH PACAP and those secondary to the doubling of adipose mass. Therefore, we clamped mice at 4 weeks post-injection before the onset of obesity, using a similar experimental design. At the time of hyperinsulinemic/euglycemic clamp, body weight, fat mass, and lean mass were not different in *Adcyap1*<sup>MBH</sup> KO mice compared to controls (Figure 7A-C). Glucose clearance and hepatic glucose production were comparable in *Adcyap1*<sup>MBH</sup> KO mice and controls (Figure 7E-L). These data indicate that three weeks post-injection and before changes in body weight and adiposity, *Adcyap1*<sup>MBH</sup> KO have normal glucose homeostasis. Together, these data indicate a nuanced role for PACAP in a metabolically stressed system.

### **Discussion**

Body energy homeostasis results from balancing energy intake and energy expenditure. In these studies, we investigated the role of PACAP in the MBH in regulating energy homeostasis. MBH neurons control metabolic function via the sympathetic nervous system according to metabolic cues such as fasting, and PACAP is a neuropeptide expressed within this area known to play an important role in metabolic control. We tested a role for MBH PACAP in multiple modalities of energy balance by using VMN-directed AAV<sup>Cre</sup> injections to ablate *Adcyap1*. Our data demonstrate that MBH PACAP is a necessary modulator of energy balance, and mice lacking PACAP expression in the MBH show severe obesity. It is important to note that obesity in *Adcyap1*<sup>MBH</sup> KO was observed on a normal

chow diet. Few studies have revealed this degree of obesity (over 50% increase in body weight and adipose mass) without an increase in food intake or accompanied by high fat diet. This is the first study to demonstrate a distinct function for PACAP in VMH and surrounding MBH cells, which help to clarify the overall metabolic function of both this hypothalamic region and PACAP. While the MBH and PACAP are each involved in glycemic control, our findings indicate that these functions are mediated by non-PACAP initiated signaling in VMN cells and PACAP-initiated signaling originating from likely non-VMN cells.

It is important to point out that neither the PACAP-KO and PAC1R-KO have been found to have this obesity phenotype (46,48-50), though both were originally generated to pursue this expected outcome. This may be because PACAP plays important but distinct role in the periphery and the CNS that may compensate metabolically. For instance, PACAP is necessary for both proper development and critical physiologic functions (46,51,52), separate from energy balance, which make it difficult to define the function for this peptide using traditional knockout approaches. In fact, 50-70% of total knockouts of either the peptide or receptor do not survive post-natal weaning (15,16). Alternatively, there may be a separate function for PACAP in other parts of the brain or periphery that may counteract with these effects via MBH cells. Peripheral PACAP and central PACAP may play separate roles in overall metabolic function that may be able to compensate for an effect observed with pharmacologic administration, but not the knockouts. There is precedent for this type of effect in metabolic function, as seen in the neural POMC-KO that has a larger effect on obesity than the global KO, rising from the HPA axis dysfunction (53).

While the roles of PACAP administration, blockade, and knockout models in the control of energy balance have been well established (52,54,55), little is known about the role of this peptide in individual sets of cells within either the brain or the periphery. A recent study showed that PACAP controls reproductive function via cells in the ventral premammillary nucleus (21) by using PMV specific PACAP knockdown. In addition to reproductive function, PACAP-containing preoptic area neurons maintain thermoregulation (56) and neurons in the paraventricular nucleus of the

hypothalamus can promote food intake (30). Both of these discoveries utilized remote activation of the respective populations using DREADD hM3dq rather than manipulating PACAP directly. Since the *Adcyap1<sup>MBH</sup>KO* mice did not exhibit deficits in fasting/re-feeding food intake (Figure 3), these may be site-specific or cell-specific functions of PACAP-expressing neurons. Thus, other PACAP-containing cells likely generate separate functions involved in whole body energy metabolism, and there may be multiple PACAP-expressing neuronal subpopulations involved in separate functions organized within the VMN. But collectively, these results suggest that the overall function of PACAP in the VMN is to appropriately respond to metabolic stressors to flexibly manage energy stores, and does so through different circuits, on different time scales, and using multiple energy balance related effectors.

Our results support the hypothesis that MBH PACAP is required to maintain proper energy balance. Particularly, rises in  $VO_2$  and  $VCO_2$  in the first four hours of the dark cycle are absent in the *Adcyap1<sup>MBH</sup>KO* mice, consistent with a defect in diet-induced thermogenesis (57). Energy expenditure, in the mouse, is primarily driven by brown adipose tissue. Brown Adipose Tissue (BAT) thermogenesis is highly regulated by the CNS, the main source of thermoregulation in the body. Several studies have identified novel neuronal circuits that control brown adipocyte thermogenesis in rodents (58-60). BAT thermogenesis has also been shown to have many positive metabolic effects, such as increased glucose and lipid uptake and decrease in body weight (61). In addition, *Adcyap1<sup>MBH</sup>KO* mice displayed markedly flat levels of fat oxidation and glucose oxidation shortly after lights off, particularly early in obesity (Figure 4). This pattern of increased fat oxidation and minimal shift toward glucose oxidation is consistent with metabolic inflexibility, a key effector for obesity (62-64). Importantly, these findings were supported by both the increased markers of fat oxidation in the BAT (Supp Fig 4) and reduced glucose uptake in the glucose clamps (Figure 6) (22). However, all of these effects were observed when knockout mice had more adipose tissue than the controls. Therefore, it makes it difficult to distinguish the cause of obesity from the effect of obesity. These mechanisms need to be further investigated at different timepoints, and perhaps with more

circumscribed subpopulations, to decipher the potential function for PACAP in the MBH in diet-induced thermogenesis and metabolic flexibility.

Non-obese *Adcyap1*<sup>MBH</sup>*KO* mice displayed normal glucose, insulin, and glucose clearance but obese *Adcyap1*<sup>MBH</sup>*KO* mice exhibited dramatic hyperinsulinemia, hyperglycemia, and suppressed glucose clearance (Figures 5 and 6). These results do not support a direct role for MBH PACAP in glucose homeostasis and may instead play a permissive role in the onset of hyperglycemia associated with obesity. However, it is interesting that insulin sensitivity was not diminished in obese *Adcyap1*<sup>MBH</sup>*KO* mice despite hyperinsulinemia and hyperglycemia, which may facilitate dysfunctional glucose uptake and suppress glucose production. There may be something unique to a chronic loss of this peptide that leads to suppressed glucose clearance, while the individual remains insulin tolerant. Distinctions within these obese models may provide explanation for the separate clinical presentation of obesity and diabetes and may shed light on therapeutics that may be effective at restoring energy balance and glucose homeostasis due to separate underlying dysfunctions. Nevertheless, dysfunctions in glucose homeostasis merely describe distinctions in this particular obese model and do not reveal direct effects by MBH PACAP. However, this unique collection of effects on glucose uptake and insulin tolerance should be investigated further in order to understand the distinctions between specific models of obesity-associated diabetes.

Our data complement and extend known functions of PACAP in VMN cells. We provide evidence that these cells can induce BAT thermogenesis. Therefore, downregulation of PACAP due to fasting and loss of leptin function likely suppresses appropriate energy expenditure. In addition, it was recently demonstrated that these VMN cells, using the same *Adcyap1*<sup>cre</sup> mouse model, are glucose-inhibited and that activation is sufficient to elevate glucose excursion in response to intraperitoneal glucose challenge (40). However, our data demonstrate that this is likely a function for non-PACAP transmitters in these VMN cells. For example, almost all VMN cells contain glutamate, which is essential for the generation of the counterregulatory response to hypoglycemia (18), indicating that VMN PACAP cells may instead use glutamate to stimulate counterregulation.

Furthermore, PACAP may play important roles in both glucose-excited and glucose-inhibited cells in the MBH, which may cancel each other out in our method of *Adcyap1* ablation. Clearly, more investigation is needed to fully understand the underlying mechanisms in the VMN that contribute to the control of overall metabolic function.

While powerful for ensuring only CNS ablation of *Adcyap1*, AAV<sup>Cre</sup> injections carry an inherent limitation that, in order to obtain significant loss of function within a given nucleus, injections will spill over into neighboring regions. While the injections were VMN-directed, we did observe GFP-labeled cells, indicating Cre-activity, in the DMH, PH, AHA, and arcuate nucleus. However, *Adcyap1* mRNA signal was not above background in these areas, as observed by other investigators as well (8,65), that indicate either modest PACAP expression within these cells or extremely small populations of PACAP. The VMN contains robust *Adcyap1* expression that is responsive to both loss of leptin and fasting conditions (8). Furthermore, these data are strikingly similar to recent data that silencing all VMN-SF1 cells results in similarly obesity and reduced energy expenditure (66). Additionally, VMN-specific knockout of either brain derived neurotrophic factor (67), thyroid hormone receptor  $\beta$  (68), or leptin receptor (20) all produce a similar, albeit less dramatic, obesity compared to *Adcyap1*<sup>MBH</sup> KO mice. However, VMN-specific glutamate knockout induces obesity due to hyperphagia, unlike *Adcyap1*<sup>MBH</sup> KO mice (18). While these data may not be dependent on VMN knockout alone, there is a considerable amount of evidence that PACAP in the VMN plays a critical role in energy balance.

Overall, these studies support an important role for PACAP within MBH cells in the control of energy balance via direct effects on body weight and BAT-related energy expenditure, but no direct effect on glucose homeostasis. MBH PACAP is required for normal energy balance, and a lack of PACAP signaling in MBH cells results in obesity. However, the MBH is a heterogeneous collection of cells that have a diverse set of functions and signals that these cells respond to (8,20,66,68-72). Recent data has made it abundantly clear that there are key subpopulations in the VMN and ARC that play distinct and sometimes opposing functions (66,73-75). Therefore, there may be important

effects of PACAP within individual subpopulations of MBH cells that offset each other, thus further studies are required to define the function of PACAP within the different populations of MBH neurons. This type of diversity in function is clearly the case in comparing CNS versus peripheral functions for neuropeptides such as PACAP. We may be underestimating the contribution of certain neuropeptides, like PACAP, that play critical roles in a specific function in a circuit-defined set of cells. Future studies will determine the precise mechanisms for these effects, including downstream signaling targets, tissues utilized for promoting energy expenditure, and effects on adipose tissue depots.

Accepted Manuscript

**Author contributions:** JNF, RR, and NBK collected and analyzed the data. JNF, NBK, BL, DJ, DLH, and RR designed experiments. BL and RR generated *Adcyap1<sup>flox</sup>* mouse model and provided feedback on studies. All authors reviewed and edited the manuscript. JNF is the guarantor of the manuscript.

**Acknowledgements:** We thank Martin G. Myers Jr., David P. Olson, Paula Goforth, Alex Banks, and Jon Resch for helpful discussions. We thank the Michigan Diabetes Center (NIH P30 DK020572, including the Molecular Genetics, Animal Studies, and Microscopy, Imaging, and Cellular Physiology Cores). We thank the University of Michigan Animal Phenotyping Core (1U2CDK110678-01). We would also like to thank the American Diabetes Association (17-INI-15 to JNF) and the Michigan Diabetes Center Pilot and Feasibility Grant for the funding to support this project. Lastly, we would like to thank the NIH (P30 DK046200, P30 DK057521, R01 DK075632, R01 DK089044, R01 DK096010, R01 DK111401 to BL, 5T32DK108740 to NBK, K08 DK118201 and T32 HL007374 to RR, and 5T32AA007462 to DLH) for funding to support this project.

**The data in this manuscript are available with reasonable request to the corresponding author.**

Accepted Manuscript

## Bibliography

1. Ogden CL, Yanovski SZ, Carroll MD, Flegal KM. The epidemiology of obesity. *Gastroenterology*. 2007;132(6):2087-2102.
2. Finkelstein EA, Trogon JG, Cohen JW, Dietz W. Annual medical spending attributable to obesity: payer-and service-specific estimates. *Health Aff (Millwood)*. 2009;28(5):w822-831.
3. Srivastava G, Apovian CM. Current pharmacotherapy for obesity. *Nat Rev Endocrinol*. 2018;14(1):12-24.
4. Comerma-Steffensen S, Grann M, Andersen CU, Rungby J, Simonsen U. Cardiovascular effects of current and future anti-obesity drugs. *Curr Vasc Pharmacol*. 2014;12(3):493-504.
5. Moreira FA, Crippa JA. The psychiatric side-effects of rimonabant. *Rev Bras Psiquiatr*. 2009;31(2):145-153.
6. Roh E, Song DK, Kim MS. Emerging role of the brain in the homeostatic regulation of energy and glucose metabolism. *Exp Mol Med*. 2016;48:e216.
7. Munzberg H, Qualls-Creekmore E, Berthoud HR, Morrison CD, Yu S. Neural Control of Energy Expenditure. *Handb Exp Pharmacol*. 2016;233:173-194.
8. Hawke Z, Ivanov TR, Bechtold DA, Dhillon H, Lowell BB, Luckman SM. PACAP neurons in the hypothalamic ventromedial nucleus are targets of central leptin signaling. *J Neurosci*. 2009;29(47):14828-14835.
9. Tanida M, Hayata A, Shintani N, Yamamoto N, Kurata Y, Shibamoto T, Morgan DA, Rahmouni K, Hashimoto H. Central PACAP mediates the sympathetic effects of leptin in a tissue-specific manner. *Neuroscience*. 2013;238:297-304.
10. Tanida M, Shintani N, Morita Y, Tsukiyama N, Hatanaka M, Hashimoto H, Sawai H, Baba A, Nagai K. Regulation of autonomic nerve activities by central pituitary adenylate cyclase-activating polypeptide. *Regul Pept*. 2010;161(1-3):73-80.
11. Hatanaka M, Tanida M, Shintani N, Isojima Y, Kawaguchi C, Hashimoto H, Kakuda M, Haba R, Nagai K, Baba A. Lack of light-induced elevation of renal sympathetic nerve activity and plasma corticosterone levels in PACAP-deficient mice. *Neurosci Lett*. 2008;444(2):153-156.
12. Yi CX, Sun N, Ackermans MT, Alkemade A, Foppen E, Shi J, Serlie MJ, Buijs RM, Fliers E, Kalsbeek A. Pituitary adenylate cyclase-activating polypeptide stimulates glucose production via the hepatic sympathetic innervation in rats. *Diabetes*. 2010;59(7):1591-1600.
13. Sekar R, Wang L, Chow BK. Central Control of Feeding Behavior by the Secretin, PACAP, and Glucagon Family of Peptides. *Front Endocrinol (Lausanne)*. 2017;8:18.
14. Diane A, Nikolic N, Rudecki AP, King SM, Bowie DJ, Gray SL. PACAP is essential for the adaptive thermogenic response of brown adipose tissue to cold exposure. *J Endocrinol*. 2014;222(3):327-339.
15. Hashimoto H, Shintani N, Baba A. Higher brain functions of PACAP and a homologous *Drosophila* memory gene amnesiac: insights from knockouts and mutants. *Biochem Biophys Res Commun*. 2002;297(3):427-431.
16. Hamelink C, Tjurmina O, Damadzic R, Young WS, Weihe E, Lee HW, Eiden LE. Pituitary adenylate cyclase-activating polypeptide is a sympathoadrenal neurotransmitter involved in catecholamine regulation and glucohomeostasis. *Proc Natl Acad Sci U S A*. 2002;99(1):461-466.

17. Meek TH, Nelson JT, Matsen ME, Dorfman MD, Guyenet SJ, Damian V, Allison MB, Scarlett JM, Nguyen HT, Thaler JP, Olson DP, Myers MG, Jr., Schwartz MW, Morton GJ. Functional identification of a neurocircuit regulating blood glucose. *Proc Natl Acad Sci U S A*. 2016;113(14):E2073-2082.
18. Tong Q, Ye C, McCrimmon RJ, Dhillon H, Choi B, Kramer MD, Yu J, Yang Z, Christiansen LM, Lee CE, Choi CS, Zigman JM, Shulman GI, Sherwin RS, Elmquist JK, Lowell BB. Synaptic glutamate release by ventromedial hypothalamic neurons is part of the neurocircuitry that prevents hypoglycemia. *Cell Metab*. 2007;5(5):383-393.
19. A Q, R K, J F, V S, Z S, S J. Assessment of epicardial fat thickness in patients with primary hypothyroidism. *J Assoc Physicians India*. 2016;64(1):44.
20. Dhillon H, Zigman JM, Ye C, Lee CE, McGovern RA, Tang V, Kenny CD, Christiansen LM, White RD, Edelstein EA, Coppari R, Balthasar N, Cowley MA, Chua S, Jr., Elmquist JK, Lowell BB. Leptin directly activates SF1 neurons in the VMH, and this action by leptin is required for normal body-weight homeostasis. *Neuron*. 2006;49(2):191-203.
21. Ross RA, Leon S, Madara JC, Schafer D, Fergani C, Maguire CA, Verstegen AM, Brengle E, Kong D, Herbison AE, Kaiser UB, Lowell BB, Navarro VM. PACAP neurons in the ventral premammillary nucleus regulate reproductive function in the female mouse. *Elife*. 2018;7.
22. [https://figshare.com/articles/figure/Supplemental\\_Figures/13477542](https://figshare.com/articles/figure/Supplemental_Figures/13477542).
23. Weir JB. New methods for calculating metabolic rate with special reference to protein metabolism. *J Physiol*. 1949;109(1-2):1-9.
24. RRID:AB\_2783839. Glucagon ELISA Kit. (*Mercodia Cat# 10-1281-01*, RRID:AB\_2783839).[http://antibodyregistry.org/AB\\_2783839](http://antibodyregistry.org/AB_2783839).
25. RRID:AB\_2722664. Mouse Leptin ELISA Kit. (*Crystal Chem Cat# 90030*, RRID:AB\_2722664).[http://antibodyregistry.org/AB\\_2722664](http://antibodyregistry.org/AB_2722664).
26. RRID:AB\_2783626. Ultra Sensitive Mouse Insulin ELISA Kit. (*Crystal Chem Cat# 90080*, RRID:AB\_2783626).[http://antibodyregistry.org/AB\\_2783626](http://antibodyregistry.org/AB_2783626).
27. RRID:AB\_2801269. Corticosterone Antiserum for 3H Assay (Rabbit) Kit. (*MP Bio Cat# 07120016*, RRID:AB\_2801269).[http://antibodyregistry.org/AB\\_2801269](http://antibodyregistry.org/AB_2801269).
28. Flak JN, Patterson CM, Garfield AS, D'Agostino G, Goforth PB, Sutton AK, Malec PA, Wong JT, Germani M, Jones JC, Rajala M, Satin L, Rhodes CJ, Olson DP, Kennedy RT, Heisler LK, Myers MG, Jr. Leptin-inhibited PBN neurons enhance responses to hypoglycemia in negative energy balance. *Nat Neurosci*. 2014;17(12):1744-1750.
29. Fenselau H, Campbell JN, Verstegen AM, Madara JC, Xu J, Shah BP, Resch JM, Yang Z, Mandelblat-Cerf Y, Livneh Y, Lowell BB. A rapidly acting glutamatergic ARC-->PVH satiety circuit postsynaptically regulated by alpha-MSH. *Nat Neurosci*. 2017;20(1):42-51.
30. Krashes MJ, Shah BP, Madara JC, Olson DP, Strohlic DE, Garfield AS, Vong L, Pei H, Watabe-Uchida M, Uchida N, Liberles SD, Lowell BB. An excitatory paraventricular nucleus to AgRP neuron circuit that drives hunger. *Nature*. 2014;507(7491):238-242.
31. Flak JN, Arble D, Pan W, Patterson C, Lanigan T, Goforth PB, Sacksner J, Joosten M, Morgan DA, Allison MB, Hayes J, Feldman E, Seeley RJ, Olson DP, Rahmouni K, Myers MG, Jr. A leptin-regulated circuit controls glucose mobilization during noxious stimuli. *The Journal of clinical investigation*. 2017;127(8):3103-3113.

32. Flak JN, Patterson CM, Garfield AS, D'Agostino G, Goforth PB, Sutton AK, Malec PA, Wong JM, Germani M, Jones JC, Rajala M, Satin L, Rhodes CJ, Olson DP, Kennedy RT, Heisler LK, Myers MG, Jr. Leptin-inhibited PBN neurons enhance responses to hypoglycemia in negative energy balance. *Nature neuroscience*. 2014;17(12):1744-1750.
33. RRID:AB\_10000240. Green Fluorescent Protein (GFP) Antibody, Aves Labs. (*Aves Labs Cat# GFP-1020*).[http://antibodyregistry.org/AB\\_10000240](http://antibodyregistry.org/AB_10000240)
34. RRID:AB\_10807945. Rabbit Anti-NeuN (polyclonal) Polyclonal Antibody, Unconjugated, Millipore. (*Millipore Cat# ABN78*).[http://antibodyregistry.org/AB\\_10807945](http://antibodyregistry.org/AB_10807945)
35. RRID:AB\_2307319. Living Colors® mCherry Monoclonal Antibody, Takara Bio. (*Takara Bio Cat# 632543*).[http://antibodyregistry.org/AB\\_2307319](http://antibodyregistry.org/AB_2307319)
36. Leininger GM, Opland DM, Jo YH, Faouzi M, Christensen L, Cappellucci LA, Rhodes CJ, Gnegy ME, Becker JB, Pothos EN, Seasholtz AF, Thompson RC, Myers MG, Jr. Leptin action via neurotensin neurons controls orexin, the mesolimbic dopamine system and energy balance. *Cell Metab*. 2011;14(3):313-323.
37. Leshan RL, Greenwald-Yarnell M, Patterson CM, Gonzalez IE, Myers MG, Jr. Leptin action through hypothalamic nitric oxide synthase-1-expressing neurons controls energy balance. *Nature medicine*. 2012.
38. Patterson CM, Wong JM, Leininger GM, Allison MB, Mabrouk OS, Kasper CL, Gonzalez IE, Mackenzie A, Jones JC, Kennedy RT, Myers MG, Jr. Ventral tegmental area neurotensin signaling links the lateral hypothalamus to locomotor activity and striatal dopamine efflux in male mice. *Endocrinology*. 2015;156(5):1692-1700.
39. Allison MB, Patterson CM, Krashes MJ, Lowell BB, Myers MG, Jr., Olson DP. TRAP-seq defines markers for novel populations of hypothalamic and brainstem LepRb neurons. *Molecular metabolism*. 2015;4(4):299-309.
40. Khodai T, Nunn N, Worth AA, Feetham CH, Belle MDC, Piggins HD, Luckman SM. PACAP Neurons in the Ventromedial Hypothalamic Nucleus Are Glucose Inhibited and Their Selective Activation Induces Hyperglycaemia. *Front Endocrinol (Lausanne)*. 2018;9:632.
41. Rodriguez-Rodriguez R, Miralpeix C, Fosch A, Pozo M, Calderon-Dominguez M, Perpinya X, Vellvehi M, Lopez M, Herrero L, Serra D, Casals N. CPT1C in the ventromedial nucleus of the hypothalamus is necessary for brown fat thermogenesis activation in obesity. *Mol Metab*. 2019;19:75-85.
42. Orozco-Solis R, Aguilar-Arnal L, Murakami M, Peruquetti R, Ramadori G, Coppari R, Sassone-Corsi P. The Circadian Clock in the Ventromedial Hypothalamus Controls Cyclic Energy Expenditure. *Cell Metab*. 2016;23(3):467-478.
43. Kageyama H, Osaka T, Kageyama A, Kawada T, Hirano T, Oka J, Miura M, Namba Y, Ricquier D, Shioda S, Inoue S. Fasting increases gene expressions of uncoupling proteins and peroxisome proliferator-activated receptor-gamma in brown adipose tissue of ventromedial hypothalamus-lesioned rats. *Life Sci*. 2003;72(26):3035-3046.
44. Perkins MN, Rothwell NJ, Stock MJ, Stone TW. Activation of brown adipose tissue thermogenesis by the ventromedial hypothalamus. *Nature*. 1981;289(5796):401-402.

45. Honda S, Morohashi K, Nomura M, Takeya H, Kitajima M, Omura T. Ad4BP regulating steroidogenic P-450 gene is a member of steroid hormone receptor superfamily. *J Biol Chem*. 1993;268(10):7494-7502.
46. Vaudry D, Falluel-Morel A, Bourgault S, Basille M, Burel D, Wurtz O, Fournier A, Chow BK, Hashimoto H, Galas L, Vaudry H. Pituitary adenylate cyclase-activating polypeptide and its receptors: 20 years after the discovery. *Pharmacol Rev*. 2009;61(3):283-357.
47. Gonzalez BJ, Basille M, Vaudry D, Fournier A, Vaudry H. [Pituitary adenylate cyclase-activating polypeptide]. *Ann Endocrinol (Paris)*. 1998;59(5):364-405.
48. Persson K, Ahren B. The neuropeptide PACAP contributes to the glucagon response to insulin-induced hypoglycaemia in mice. *Acta Physiol Scand*. 2002;175(1):25-28.
49. Tomimoto S, Ojika T, Shintani N, Hashimoto H, Hamagami K, Ikeda K, Nakata M, Yada T, Sakurai Y, Shimada T, Morita Y, Ishida C, Baba A. Markedly reduced white adipose tissue and increased insulin sensitivity in adcyap1-deficient mice. *J Pharmacol Sci*. 2008;107(1):41-48.
50. Nakata M, Kohno D, Shintani N, Nemoto Y, Hashimoto H, Baba A, Yada T. PACAP deficient mice display reduced carbohydrate intake and PACAP activates NPY-containing neurons in the rat hypothalamic arcuate nucleus. *Neurosci Lett*. 2004;370(2-3):252-256.
51. Shen S, Gehlert DR, Collier DA. PACAP and PAC1 receptor in brain development and behavior. *Neuropeptides*. 2013;47(6):421-430.
52. Sherwood NM, Adams BA, Isaac ER, Wu S, Fradinger EA. Knocked down and out: PACAP in development, reproduction and feeding. *Peptides*. 2007;28(9):1680-1687.
53. Smart JL, Tolle V, Low MJ. Glucocorticoids exacerbate obesity and insulin resistance in neuron-specific proopiomelanocortin-deficient mice. *J Clin Invest*. 2006;116(2):495-505.
54. Nakata M, Yada T. PACAP in the glucose and energy homeostasis: physiological role and therapeutic potential. *Curr Pharm Des*. 2007;13(11):1105-1112.
55. Matsuda K, Maruyama K. Regulation of feeding behavior by pituitary adenylate cyclase-activating polypeptide (PACAP) and vasoactive intestinal polypeptide (VIP) in vertebrates. *Peptides*. 2007;28(9):1761-1766.
56. Tan CL, Cooke EK, Leib DE, Lin YC, Daly GE, Zimmerman CA, Knight ZA. Warm-Sensitive Neurons that Control Body Temperature. *Cell*. 2016;167(1):47-59 e15.
57. Lowell BB, Bachman ES. Beta-Adrenergic receptors, diet-induced thermogenesis, and obesity. *J Biol Chem*. 2003;278(32):29385-29388.
58. Dodd GT, Decherf S, Loh K, Simonds SE, Wiede F, Balland E, Merry TL, Munzberg H, Zhang ZY, Kahn BB, Neel BG, Bence KK, Andrews ZB, Cowley MA, Tiganis T. Leptin and insulin act on POMC neurons to promote the browning of white fat. *Cell*. 2015;160(1-2):88-104.
59. McGlashan JM, Gorecki MC, Kozlowski AE, Thirnbeck CK, Markan KR, Leslie KL, Kotas ME, Potthoff MJ, Richerson GB, Gillum MP. Central serotonergic neurons activate and recruit thermogenic brown and beige fat and regulate glucose and lipid homeostasis. *Cell Metab*. 2015;21(5):692-705.
60. Ruan HB, Dietrich MO, Liu ZW, Zimmer MR, Li MD, Singh JP, Zhang K, Yin R, Wu J, Horvath TL, Yang X. O-GlcNAc transferase enables AgRP neurons to suppress browning of white fat. *Cell*. 2014;159(2):306-317.

61. Bartelt A, Bruns OT, Reimer R, Hohenberg H, Ittrich H, Peldschus K, Kaul MG, Tromsdorf UI, Weller H, Waurisch C, Eychmuller A, Gordts PL, Rinninger F, Bruegelmann K, Freund B, Nielsen P, Merkel M, Heeren J. Brown adipose tissue activity controls triglyceride clearance. *Nat Med*. 2011;17(2):200-205.
62. Goodpaster BH, Sparks LM. Metabolic Flexibility in Health and Disease. *Cell Metab*. 2017;25(5):1027-1036.
63. Storlien L, Oakes ND, Kelley DE. Metabolic flexibility. *Proc Nutr Soc*. 2004;63(2):363-368.
64. Muoio DM. Metabolic inflexibility: when mitochondrial indecision leads to metabolic gridlock. *Cell*. 2014;159(6):1253-1262.
65. Lein ES, Hawrylycz MJ, Ao N, Ayres M, Bensinger A, Bernard A, Boe AF, Boguski MS, Brockway KS, Byrnes EJ, Chen L, Chen L, Chen TM, Chin MC, Chong J, Crook BE, Czaplinska A, Dang CN, Datta S, Dee NR, Desaki AL, Desta T, Diep E, Dolbeare TA, Donelan MJ, Dong HW, Dougherty JG, Duncan BJ, Ebbert AJ, Eichele G, Estin LK, Faber C, Facer BA, Fields R, Fischer SR, Fliss TP, Frensley C, Gates SN, Glattfelder KJ, Halverson KR, Hart MR, Hohmann JG, Howell MP, Jeung DP, Johnson RA, Karr PT, Kawal R, Kidney JM, Knapik RH, Kuan CL, Lake JH, Laramée AR, Larsen KD, Lau C, Lemon TA, Liang AJ, Liu Y, Luong LT, Michaels J, Morgan JJ, Morgan RJ, Mortrud MT, Mosqueda NF, Ng LL, Ng R, Orta GJ, Overly CC, Pak TH, Parry SE, Pathak SD, Pearson OC, Puchalski RB, Riley ZL, Rockett HR, Rowland SA, Royall JJ, Ruiz MJ, Sarno NR, Schaffnit K, Shapovalova NV, Sivisay T, Slaughterbeck CR, Smith SC, Smith KA, Smith BI, Sotdt AJ, Stewart NN, Stumpf KR, Sunkin SM, Sutram M, Tam A, Teemer CD, Thaller C, Thompson CL, Varnam LR, Visel A, Whitlock RM, Wohnoutka PE, Wolkey CK, Wong VY, Wood M, Yaylaoglu MB, Young RC, Youngstrom BL, Yuan XF, Zhang B, Zwingman TA, Jones AR. Genome-wide atlas of gene expression in the adult mouse brain. *Nature*. 2007;445(7124):168-176.
66. Flak JN, Goforth P, Dell'Orco J, Sabatini PV, Li C, Bozadjieva N, Sorensen MJ, Valenta AC, Rupp AC, Affinati AH, Cras-Meneur C, Ansari A, Sacksner J, Kodur N, Sandoval DA, Kennedy RT, Olson D, Myers MG, Jr. Ventromedial hypothalamic nucleus neuronal subset regulates blood glucose independently of insulin. *J Clin Invest*. 2020.
67. Yang H, An JJ, Sun C, Xu B. Regulation of Energy Balance via BDNF Expressed in Nonparaventricular Hypothalamic Neurons. *Mol Endocrinol*. 2016;30(5):494-503.
68. Hameed S, Patterson M, Dhillon WS, Rahman SA, Ma Y, Holton C, Gogakos A, Yeo GSH, Lam BYH, Poley-Wolf J, Fenske W, Bell J, Anastasovska J, Samarut J, Bloom SR, Bassett JHD, Williams GR, Gardiner JV. Thyroid Hormone Receptor Beta in the Ventromedial Hypothalamus Is Essential for the Physiological Regulation of Food Intake and Body Weight. *Cell Rep*. 2017;19(11):2202-2209.
69. Faber CL, Matsen ME, Velasco KR, Damian V, Phan BA, Adam D, Therattil A, Schwartz MW, Morton GJ. Distinct Neuronal Projections From the Hypothalamic Ventromedial Nucleus Mediate Glycemic and Behavioral Effects. *Diabetes*. 2018;67(12):2518-2529.
70. Hurley M, Anderson E, Chen C, Maunze B, Hess E, Block M, Patel N, Cooper Z, McCoy R, Dabra T, Conley W, Reilly M, Hearing M, Choi S. Acute blockade of PACAP-dependent activity in the ventromedial nucleus of the

- hypothalamus disrupts leptin-induced behavioral and molecular changes in rats. *Neuroendocrinology*. 2019.
71. Kunwar PS, Zelikowsky M, Remedios R, Cai H, Yilmaz M, Meister M, Anderson DJ. Ventromedial hypothalamic neurons control a defensive emotion state. *Elife*. 2015;4.
  72. Yang CF, Chiang MC, Gray DC, Prabhakaran M, Alvarado M, Juntti SA, Unger EK, Wells JA, Shah NM. Sexually dimorphic neurons in the ventromedial hypothalamus govern mating in both sexes and aggression in males. *Cell*. 2013;153(4):896-909.
  73. Routh VH. Glucosensing neurons in the ventromedial hypothalamic nucleus (VMN) and hypoglycemia-associated autonomic failure (HAAF). *Diabetes Metab Res Rev*. 2003;19(5):348-356.
  74. Campbell JN, Macosko EZ, Fenselau H, Pers TH, Lyubetskaya A, Tenen D, Goldman M, Verstegen AM, Resch JM, McCarroll SA, Rosen ED, Lowell BB, Tsai LT. A molecular census of arcuate hypothalamus and median eminence cell types. *Nat Neurosci*. 2017;20(3):484-496.
  75. Coutinho EA, Okamoto S, Ishikawa AW, Yokota S, Wada N, Hirabayashi T, Saito K, Sato T, Takagi K, Wang CC, Kobayashi K, Ogawa Y, Shioda S, Yoshimura Y, Minokoshi Y. Activation of SF1 Neurons in the Ventromedial Hypothalamus by DREADD Technology Increases Insulin Sensitivity in Peripheral Tissues. *Diabetes*. 2017;66(9):2372-2386.

Accepted Manuscript

**Figure 1. Activation of VMN *Adcyap1* cells increases BAT temperature.** We administered an AAV that introduces hM3Dq in *Adcyap1* cells in the VMN (A) and measured iBAT temperature in response to both Clozapine-n-oxide (CNO) and Saline (vehicle control) (B). Data are expressed as mean +/- SEM. Results were analyzed by two way repeated measures ANOVA. Open circles and bars refer to Saline control and closed circles and bars refer to CNO. n=5, \*p<.05

**Figure 2. AAV-cre injection ablates VMN *Adcyap1* expression.** We administered AAV-Cre into the VMN of *Adcyap1*<sup>flox</sup> mice to truncate the gene and inactivate the resultant peptide (A). This floxed mutant leads to a frameshift mutation producing a truncated protein that can no longer act on the receptor. Representative images of *in situ* hybridization for *Adcyap1* (black signal) in control AAV-GFP-injected (top panel) and AAV-cre-injected (bottom panel) mice (B). Quantification of *Adcyap1* mRNA signal in the VMN, medial amygdala (MeA), preoptic area (POA), and ventral premammillary nucleus (PMV) (C). Cell counts in the VMN were quantified (F) after staining for NeuN (D-E) in mice 12 weeks post-AAV injection. Dorsomedial Hypothalamus (DMH), Ventromedial Hypothalamic Nucleus (VMN), Arcuate Nucleus (ARC), Median Eminence (ME), and Third Ventricle (3V) are noted in the figure. Data are expressed as mean +/- SEM. Results were analyzed by student's t test. Open bars refer to GFP control and closed bars refer to Cre. n=16 (GFP), 22 (cre) in C and n=8 (GFP), 8 (Cre) in F, \*p<.05

**Figure 3. Loss of *Adcyap1* in MBH induces obesity.** Following AAV injection, we measured body weight (A) and food intake (B) for 10 weeks post-injection in male mice. We also tested the status of homeostatic feeding systems by re-feeding mice following overnight fast performed during the light cycle (C). Data are expressed as mean +/- SEM. Results were analyzed by repeated measures ANOVA with Fisher's LSD post hoc tests in A, C-D, and student's t test in B. Open circles refer to GFP control and closed circles refer to Cre. n=8 (gfp), 11 (cre), \*p<.05

**Figure 4. *Adcyap1*<sup>MBH</sup> KO mice have impaired energy expenditure measured by indirect calorimetry.** At four weeks post-injection, we measured body composition via Echo MRI (A-B). At five weeks, we weighed iBAT tissue (C). Food intake was collected in the metabolic chambers (D). VO<sub>2</sub> and VCO<sub>2</sub> were analyzed by normalizing lean mass (E,F). Respiratory exchange ratio, ambulatory activity, fat oxidation, and glucose oxidation were also measured in the metabolic chambers (I, K, M, O). In addition to data collected every 40 minutes, average values separately by light and dark cycle are also included (F,H,J,L,N,P). Data are expressed as mean +/- SEM. Results were analyzed by two-way ANOVA with Fisher's LSD post hoc tests in F, H, J, L, N, P, and repeated measures ANOVA with Fisher's LSD post hoc tests in D, F, H, J, L, N. Results were measured by student's t test in A-D. Open circles and bars refer to GFP control and closed circles and bars refer to Cre. n=5 (gfp), 7 (cre), \*p<.05

**Figure 5. *Adcyap1*<sup>MBH</sup> KO mice are hyperglycemic and hyperinsulinemic, but not insulin resistant.** In addition to body weight and food intake-related measures, we determined if glycemic factors were also out of balance. We measured glucose (A), insulin (B), glucagon (C), and corticosterone (D) at both fed and post-overnight fast. All of these tests were performed during the light cycle. We also performed glucose (2g/kg) tolerance test (E) and insulin (.6U/kg) tolerance test (F). We also

measured corticosterone (G) and glucagon (H) levels 30 minutes following insulin injection. Data are expressed as mean +/- SEM. Results were analyzed by two-way ANOVA with Fisher's LSD post hoc tests in A-D and repeated measures ANOVA with Fisher's LSD post hoc tests in E-F. Results in G-H were analyzed by student's t test. Open circles and bars refer to GFP control and closed circles and bars refer to Cre. n=16 (gfp), 22 (cre), \*p<.05

**Figure 6. Obese *Adcyap1*<sup>MBH</sup> KO mice have impaired glucose clearance.** We used the hyperinsulinemic/euglycemic clamp during the light cycle to determine whether glucose clearance was impaired in male *Adcyap1*<sup>MBH</sup> KO mice, as suggested with preliminary analysis of glycemic parameters (Figure 4). Glucose was clamped at 150 mg/dl (A). We measured glucose infusion rate (B), glucose disposal (C), and hepatic glucose production (D) both before and during the clamp. We also measured the uptake of radio-labeled 2-deoxy glucose in the muscle (E), brown adipose tissue (F), visceral fat (G), subcutaneous fat (H), and the heart (I). Data are expressed as mean +/- SEM. Results were analyzed by repeated measures ANOVA with Fisher's LSD post hoc tests in A-B, two-way ANOVA with Fisher's LSD post hoc tests in C-D, and student's t test in E-I. Open circles and bars refer to GFP control and closed squares and bars refer to Cre. n=7 (gfp), 11 (cre), \*p<.05

**Figure 7. *Adcyap1*<sup>MBH</sup> KO mice do not have impaired glucose clearance prior to obesity.** Before mice were obese, glucose clamps were performed during the light cycle in a cohort of male mice to determine the direct function of the peptide versus effects secondary to obesity. We measured body weight (A), fat mass (B), and lean mass (C) prior to clamp. Glucose was clamped at 150mg/dl (D). We measured glucose infusion rate (E). In addition, we measured glucose disposal (F) and hepatic glucose production (G) both before and during the clamp. Lastly, we measured the uptake of radio-labeled 2-deoxyglucose in the muscle (H), brown adipose tissue (I), visceral fat (J), subcutaneous fat (K), and heart (L) after the clamp. Data are expressed as mean +/- SEM. Results were analyzed by student's t test in A-C, H-K, repeated measures ANOVA with Fisher's LSD post hoc tests in D-E, and two-way ANOVA with Fisher's LSD post hoc tests in F-G. Open circles and bars refer to GFP control and closed squares and bars refer to Cre. n=5 (gfp), 7 (cre)

Accepted Article

Accer

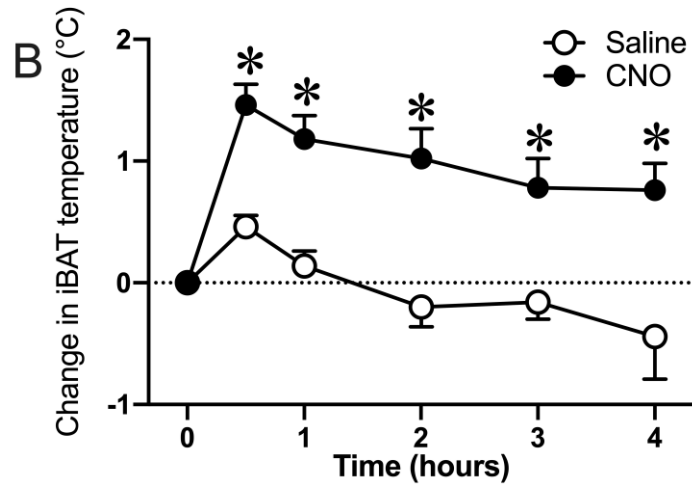
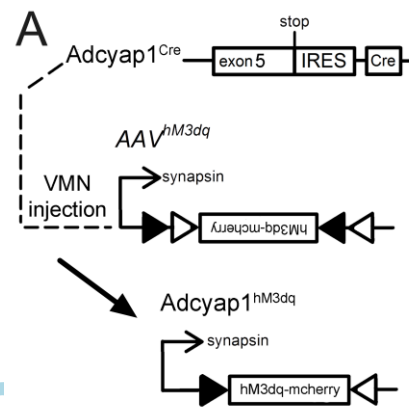
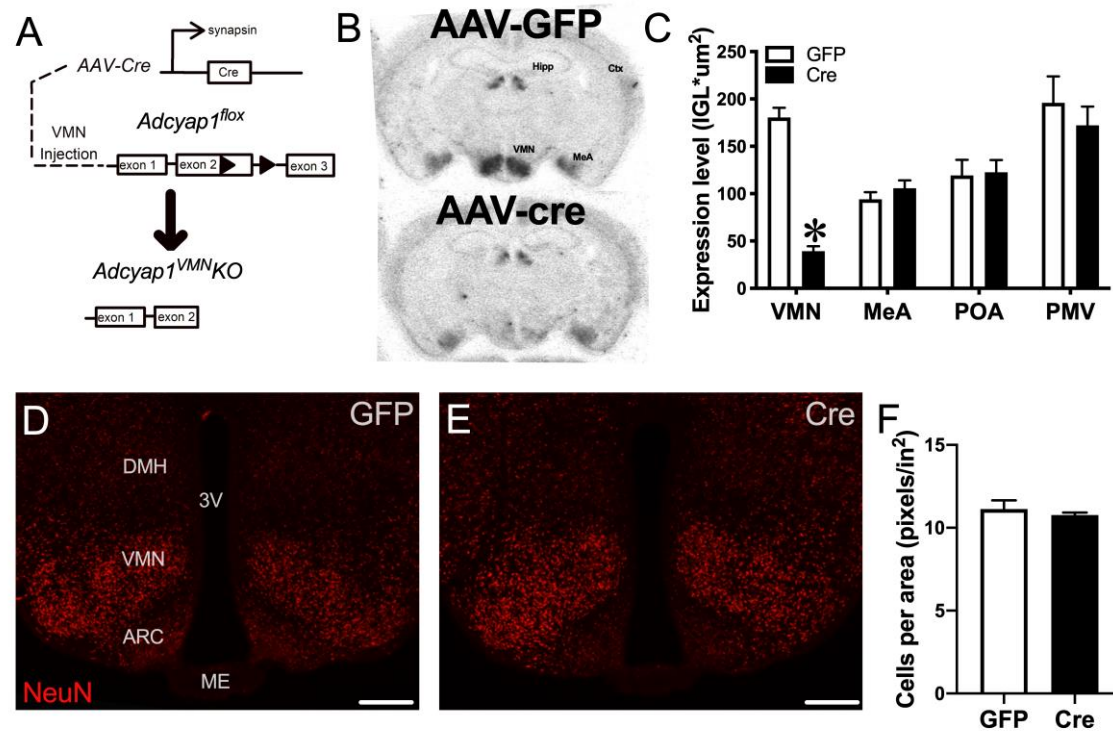


Figure 1

Figure 2



Accer

Accepted

Figure 3

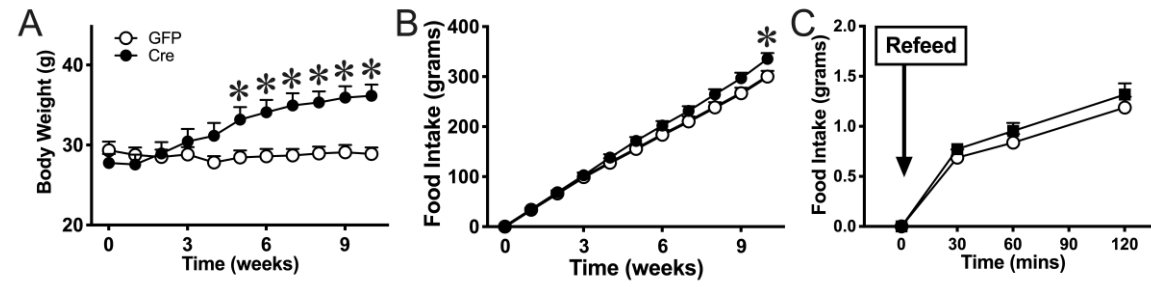


Figure 4

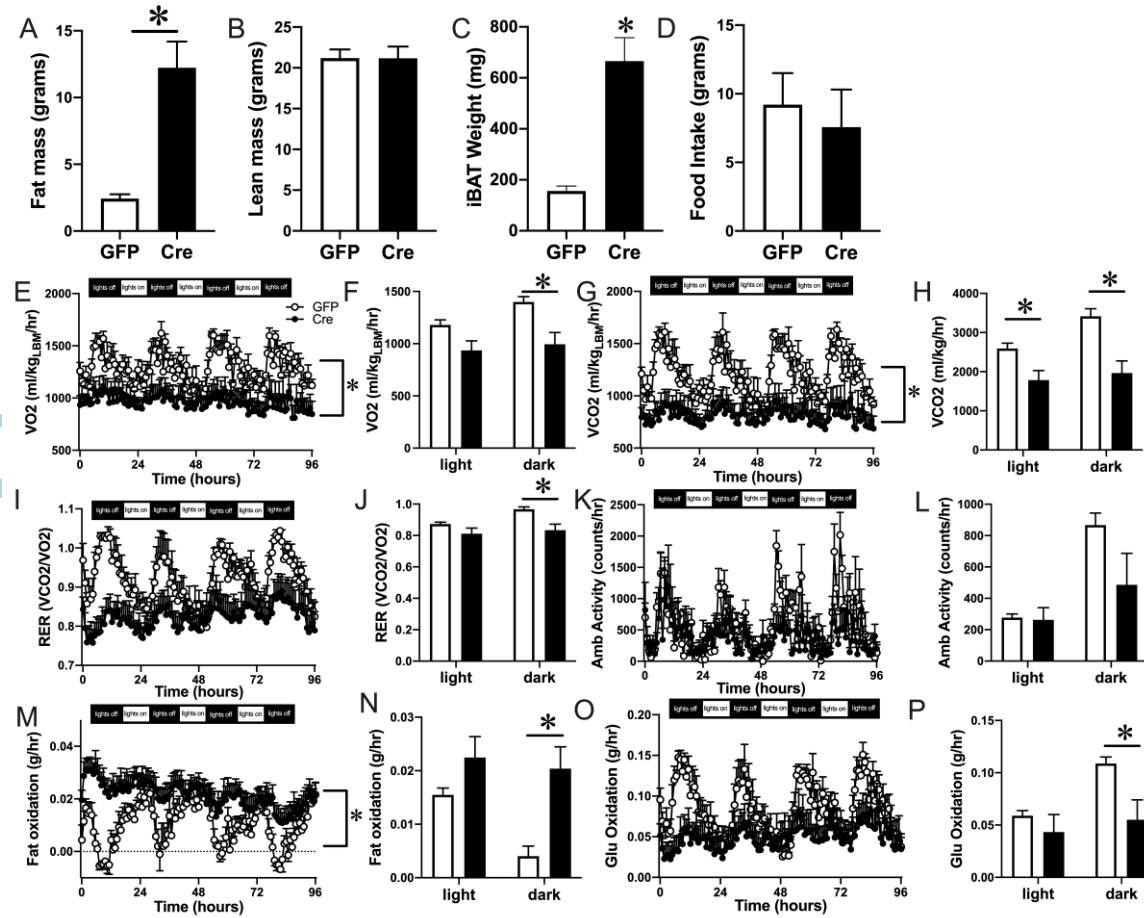
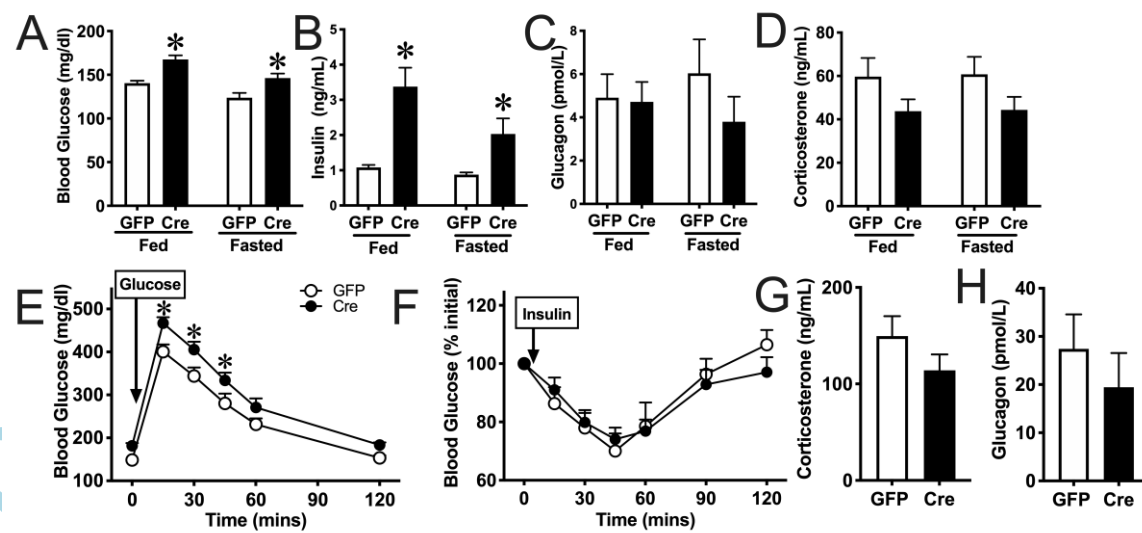


Figure 5



Accer

Figure 6

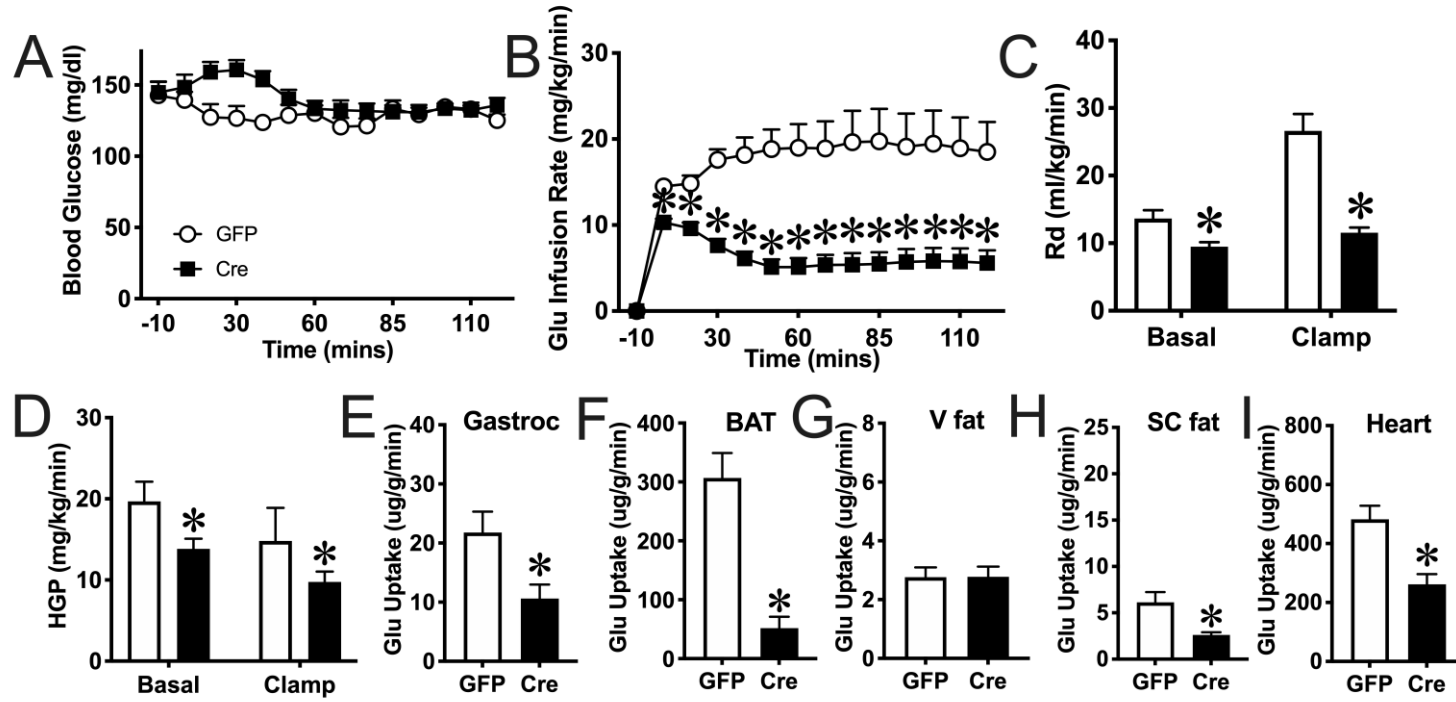


Figure 7

